ASME CODE AND RATCHETING IN PIPING COMPONENTS

DOE/NE/21746--T1

Final Technical Report
DOE Grant No.
DE-FG03-97NE21746/M002

Investigators:

Tasnim Hassan and Vernon C. Matzen

May 14, 1999

Center for Nuclear Power Plant
Structures, Equipment and Piping

North Carolina State University
Raleigh, NC 27695-7908

DISCLAIMER

DISCLAIMER

Portions of this document may be illegible in electronic image products. Images are produced from the best available original document.

ASME CODE AND RATCHETING IN PIPING COMPONENTS

Final Technical Report
DOE Grant No.
DE-FG03-97NE21746/M002

Investigators:

Tasnim Hassan and Vernon C. Matzen

May 14, 1999

Center for Nuclear Power Plant
Structures, Equipment and Piping

North Carolina State University
Raleigh, NC 27695-7908

ASME CODE AND RATCHETING IN PIPING COMPONENTS

Tasnim Hassan and Vernon C. Matzen
Center for Nuclear Power Plant Structures, Equipment and Piping
North Carolina State University
Department of Civil Engineering, Box 7908
Raleigh, NC 27695-7908

Executive Summary

The main objective of this research is to develop an analysis program which can accurately simulate ratcheting in piping components subjected to seismic or other cyclic loads. Ratcheting is defined as the accumulation of deformation in structures and materials with cycles. This phenomenon has been demonstrated to cause failure to piping components (known as ratcheting-fatigue failure) and is yet to be understood clearly. The design and analysis methods in the ASME Boiler and Pressure Vessel Code for ratcheting of piping components are not well accepted by the practicing engineering community.

This research project attempts to understand the ratcheting-fatigue failure mechanisms and improve analysis methods for ratcheting predictions. In the first step a state-of-the-art testing facility is developed for quasi-static cyclic and seismic testing of straight and elbow piping components. A systematic testing program to study ratcheting is developed. Some tests have already been performed and the rest will be completed by summer'99. Significant progress has been made in the area of constitutive modeling. A number of sophisticated constitutive models have been evaluated in terms of their simulations for a broad class of ratcheting responses. From the knowledge gained from this evaluation study two improved models are developed. These models are demonstrated to have promise in simulating ratcheting responses in piping components. Hence, implementation of these improved models in widely used finite element programs, ANSYS and/or ABAQUS, is in progress. Upon achieving improved finite element programs for simulation of ratcheting, the ASME Code provisions for ratcheting of piping components will be reviewed and more rational methods will be suggested. Also, simplified analysis methods will be developed for operability studies of piping components and systems. Some of the future works will be performed under the auspices of the Center for Nuclear Power Plant Structures, Equipment and Piping. Proposals for future funding also will be submitted to different organizations and industries to speed up the progress of the research.

ASME CODE AND RATCHETING IN PIPING COMPONENTS

I. Objectives

The objectives of this research project are:

1. Understand thoroughly the phenomenon of ratcheting by performing a systematic experimental study on materials and piping components.
2. Develop constitutive models to accurately simulate ratcheting and other cyclic responses of materials. Incorporate improved cyclic plasticity models into a commercially available finite element program to accurately simulate ratcheting responses and ultimate capacity of piping components.
3. Finally, when the ratcheting response of a piping component is sufficiently well understood and simulated
   - Develop simplified methods for analysis and design of piping components and systems.
   - Establish relationship between local and global ratcheting in piping components to develop a monitoring method for operability investigations.
   - Suggest revisions to the ASME Boiler and Pressure Vessel Code provisions for ratcheting-fatigue.

II. Research Steps

The following steps were planned over five years to achieve the objective of the proposal:

1. Acquire a state-of-the-art testing facility for quasi-static cyclic and seismic testing of piping components
2. Perform a systematic set of quasi-static cyclic testing on materials, and straight and elbow pipe components
3. Perform a systematic set of seismic tests on straight and elbow pipe components
4. Analyze the acquired test data to understand the mechanisms of fatigue-ratcheting failure
5. Develop improved constitutive models to simulate the material ratcheting responses
6. Implement the improved constitutive models into widely used finite element programs, ANSYS and/or ABAQUS, to simulate ratcheting of piping components
7. Develop simplified analysis methods for operability studies of piping components and systems
8. Review the ASME Code provisions for ratcheting of piping components using the improved finite element program; suggest more rational methods.

The proposal was funded for only one year. Due to unexpected delay in fabrication of the shake-table a six month no-cost extension was granted to the research. Despite the limited funding and one and half year of research period a significant number of accomplishments has been made as listed below.

III. Research Accomplishments

1. Test Facility

Upgrade Universal Fatigue Testing Machine

A 55 Kips MTS Load Unit and a T-Slot Table (MTS 322.31) are added to the existing MTS 458 Controller. With this set-up both quasi-static and high loading rate piping component and material tests can be performed.

Shake-Table Test Set-Up

A schematic of the shake table acquired is shown in Fig. 1. The shake table is driven with a 20 kip servo-hydraulic actuator with dual 15 GPM servo valves and controlled with a Gardner Systems GS2000 single channel servo unit which can handle random input signals with frequencies up to 40 Hz. The actuators have a 3 inch stroke, a peak velocity of 15 ips and a peak acceleration of about 5g. The displacement-controlled sled is guided by rails and can accommodate objects up to 2 ft by 4 ft in size, weighing 2,000 to 5,000 lb.

Instrumentation consists of DL Instruments Model 4302 Variable Electronic Filters (26 channels, 10Hz -1MHz), Dytran Instruments Model 3166A accelerometers (+/- 50G, response to 10 kHz), Celesco PT101 position transducers (20 inch range), and a Trans-tek 6 inch LVDT.

2. Test Program

A set of quasi-static and seismic responses of stainless steel (SS) 304 straight and elbow piping components subjected to various levels of internal pressure and cyclic bending will be studied. Experiments will be performed with five different test set-up as listed below:

1. quasi-static cyclic bending of straight pipe (Fig. 2a),
2. quasi-static in-plane cyclic bending of elbow pipe (Fig. 2b),
3. quasi-static out-of-plane cyclic bending of elbow pipe (Fig. 2c),
4. seismic testing of straight pipe (Fig. 3),
5. seismic testing of elbow pipe (Fig. 4).

The tests in Fig. 2 will be performed in the universal fatigue testing machine and those in Figs. 3 and 4 on the shake table. A series of material ratcheting tests will be performed on SS304 straight pipes by prescribing various stress and strain histories using the testing machine and a servo-controlled cyclic pressurization device.

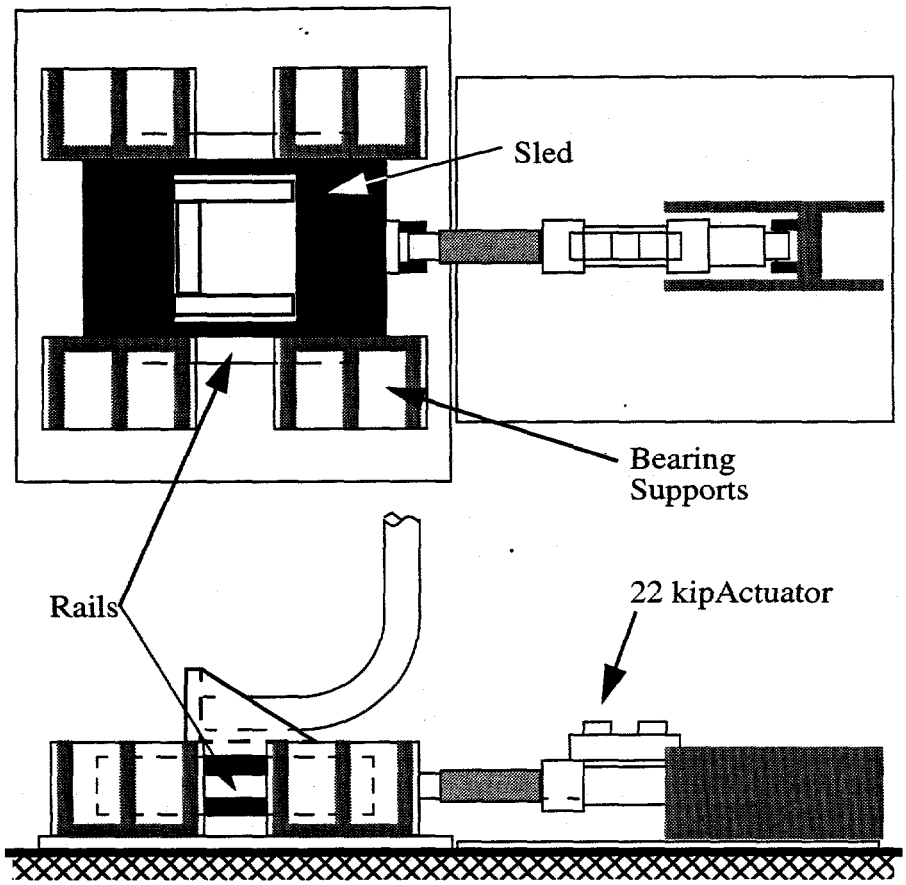

Fig. 1. NCSU Shake-table set-up

Specimen

Long radius elbow and straight piping components of 2 inches nominal diameter and schedule 10 thickness will be used as test specimens. Straight pipe segments, of the same material and the same cross-sectional dimensions, will be welded to the ends of the elbow specimens to reduce the end effect on the measured data.

3. Tests Performed

Several elbow component tests and material tests have been performed so far. The remaining tests in the program will be performed in the summer of 1999 through a project of the Center for Nuclear Power Plant Structures, Equipment and Piping.

Strain Gage Study

Due to the occurrence of strain shift in gages during cyclic loading, three types of strain gages are evaluated to determine the best gage suited for measuring ratcheting strains. In this

study a uniaxial ratcheting experiment is performed and the ratcheting strains are measured using EP, EA-rosette, CEA stacked and tee type gages and also using an extensometer.

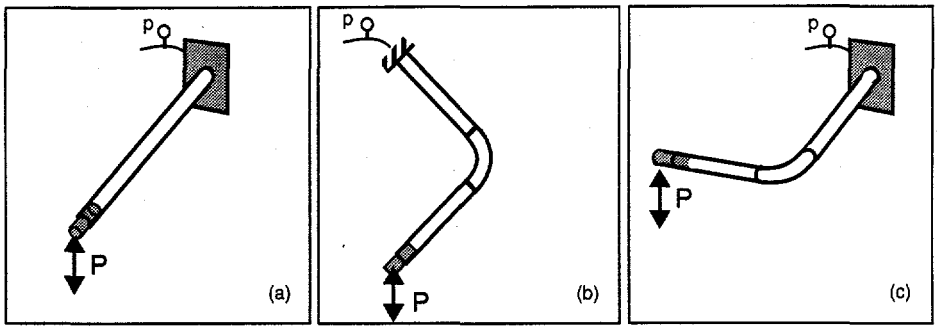

Fig. 2. Test set-up. (a) Straight pipe cantilever, (b) in-plane bending of elbow, (c) out-of-plane bending of elbow and bending/torsion of straight pipe

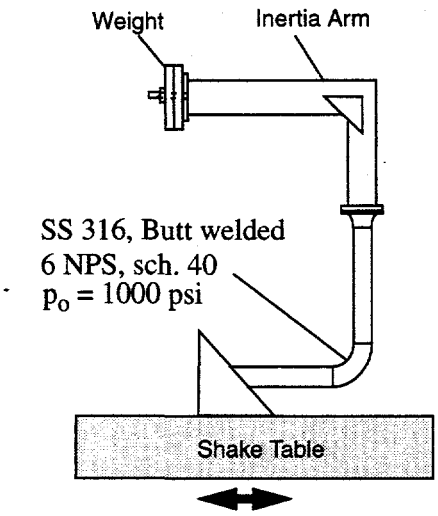

Fig. 3. Shake-table elbow component test set-up

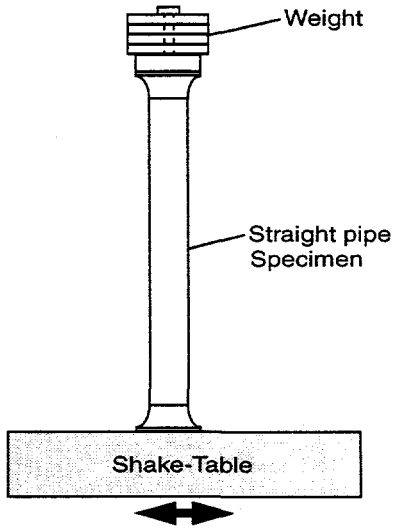

Fig. 4. Straight pipe shake-table test set-up

The data from the experiment are plotted in Fig. 5, where the maximum strain in each cycle is plotted as a function of the number of cycles. The strain data from extensometer is considered to be accurate and compared with the strain gage data to evaluate gage performance. In Fig. 5, we see that the CEA and EA gages perform the best in measuring ratcheting strains up to 2%, after which the gages came off the pipe. These stacked, rosette and tee gages are stiff compare to a single gage and hence striped off the curved surface at a small strain level. The single CEA performed better in ratcheting tests and hence we decided to use the CEA single gage in our study.

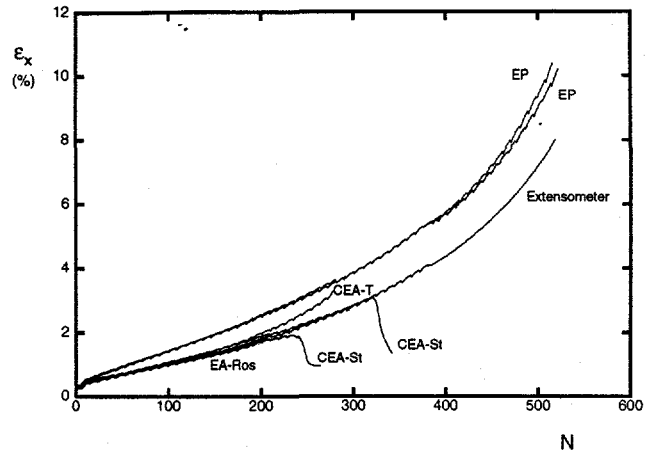

Fig. 5. Evaluation of strain gages for measuring ratcheting strains

Elbow Monotonic Opening and Closing Tests

Two tests, one monotonic opening test and one monotonic closing test, both displacement controlled, are perform in order to determine the parameters for in-plane cyclic bending tests. The results from these tests are shown in Fig. 5. The response in opening mode gradually stiffens due to increase in moment of inertia of the cross-section, whereas that in closing mode softens due to decrease in moment of inertia of the cross-section. This decrease and increase in moment of inertia resulted from ovalization of the cross-section. The results from these monotonic tests are also used in another project of the Center for Nuclear Power Plant Structures, Equipment and Piping entitled "B Stress Indices Using Finite Element Analysis."

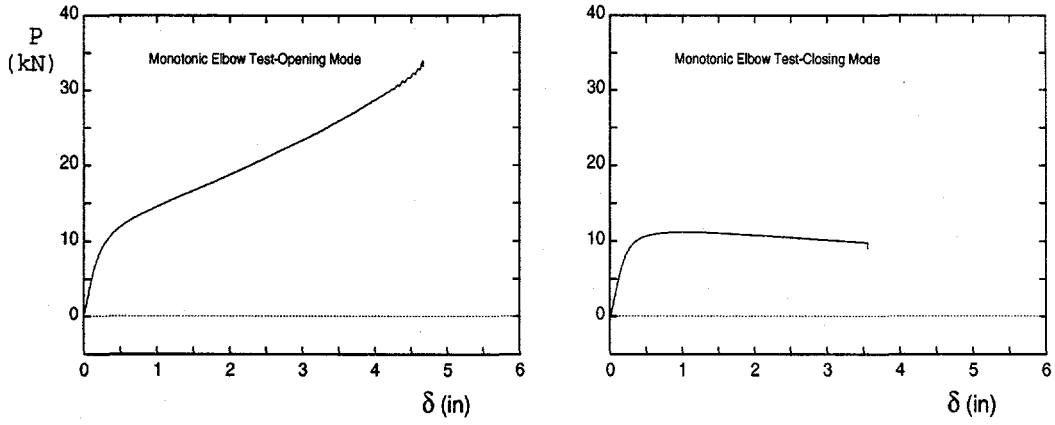

Fig. 5. Monotonic opening and closing responses of elbow component

Elbow In-Plane Cyclic Bending Tests

An elbow test by prescribing opening-closing displacement-controlled cycles in the presence of internal pressure is performed. The displacement cycles involve five different amplitudes ± 0.2", 0.3", 0.4", 0.5" and 0.6". The internal pressure prescribed in the test is 710 psi.

The force-displacement response in the test is shown in Fig. 6. Note in this figure that the force-displacement response during opening cycles is stiffer than during closing cycles. This difference in responses again is the result of changes in the moment of inertia due to cross-section ovalization.

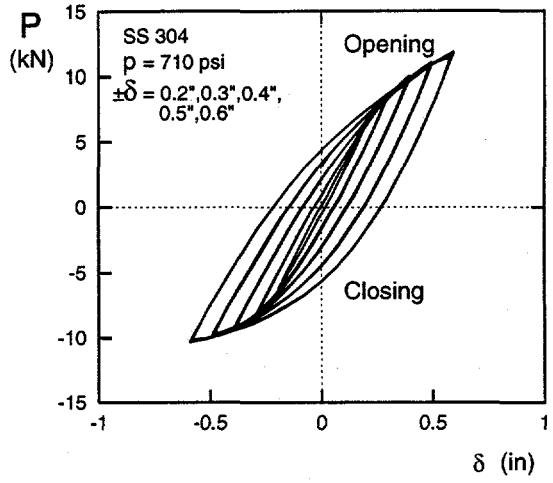

Fig. 6. force-displacement response in cyclic elbow test

The axial and hoop strain responses at flank, intrados and extrados in the cyclic bending test of elbow are shown in Fig. 7. In the first step, where the displacement amplitude is ±0.2", the resulting strains are in the elastic range, hence ratcheting does not occur at any location. As the displacement amplitude is increased to ±0.3" the materials at these locations enter the inelastic range and the hoop strains start ratcheting. The rates of hoop strain ratcheting at the intrados and extrados are very small, and that at the flank is larger and noticeable. The axial strain at intrados shows a little ratcheting in the negative direction, whereas at the other two locations no sign of axial ratcheting is observed. The reason of small amplitude axial strain cycles at the extrados is the cancellation of tensile axial strain by the compressive bending strain and vice versa. The rates of hoop strain ratcheting gradually increase with increase in amplitudes of displacement cycles.

A set of similar experiments with different experimental parameters will be performed and critically analyzed in order to understand ratcheting-fatigue failure mechanisms in elbow components and for verification of the improved analysis programs. As mentioned earlier these test set will be completed in summer of 1999.

4. Constitutive Modeling

Significant progress has been made in constitutive modeling for ratcheting through this research. The performance of several sophisticated constitutive models in predicting ratcheting responses of metallic materials for a series of uniaxial and biaxial experiments is evaluated. The models proposed by Chaboche [1986, 1991, 1994], Ohno [1993a,b, 1997], Guionnet [1992] and modified Dafalias-Popov [Hassan and Kyriakides, 1992, Hassan et al., 1992] are examined. Using the knowledge gained from the evaluation improved models are developed for better simulation of ratcheting.

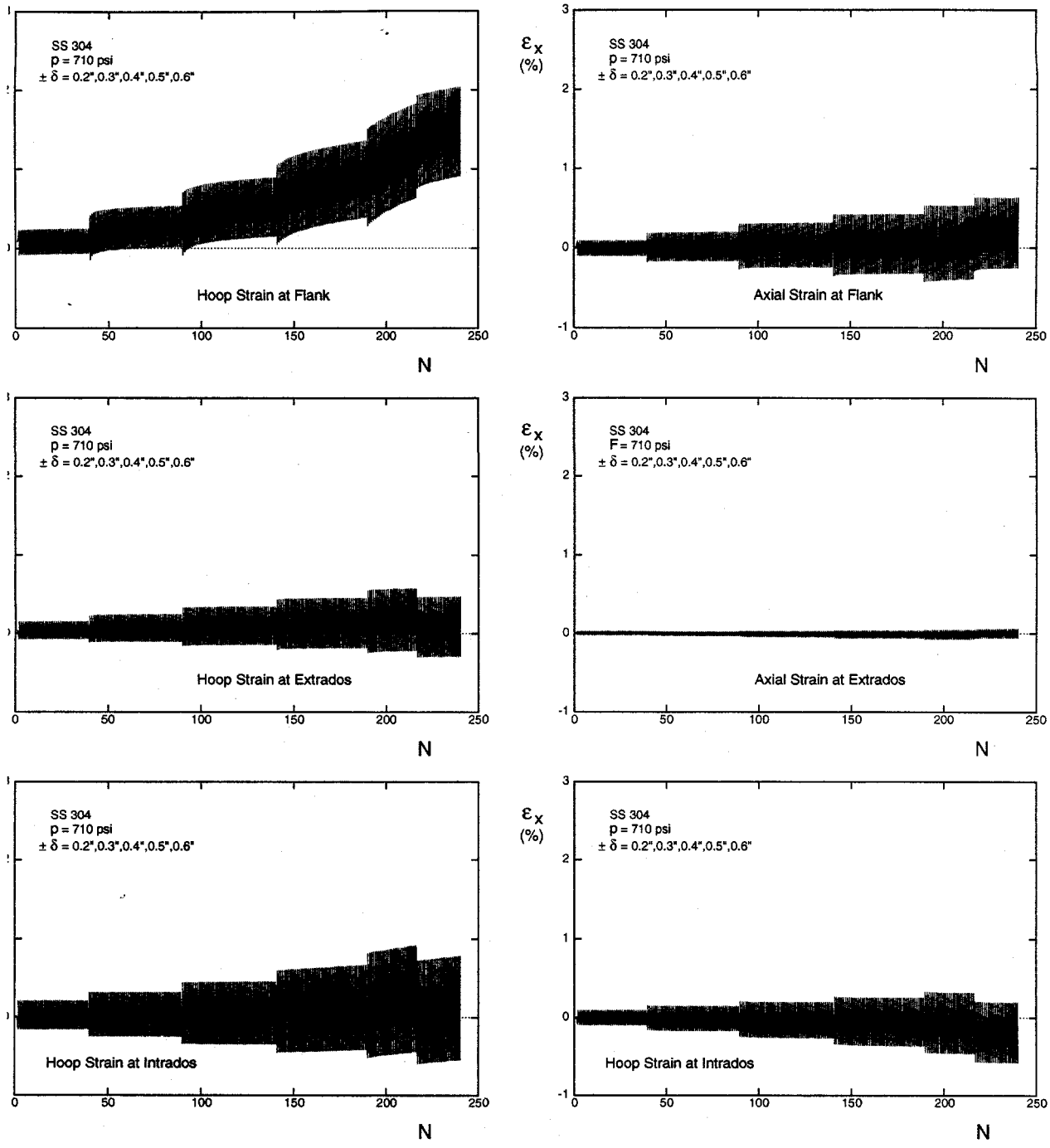

Fig. 7. Axial and hoop strain responses in the cycling bending of elbow experiment at extrados, intrados and flank.

Material Responses Studied

Ratcheting responses from four different loading histories (see Fig. 8) are considered for validating constitutive models. These responses include one set of uniaxial and three sets of biaxial ratcheting responses of carbon steel 1026 or 1018 (CS 1026 or CS1018). These data were collected from the works of Hassan and Kyriakides [1992], Hassan et al. [1992] and Corona et al. [1996]. The uniaxial ratcheting experiment involved stress cycling with constant amplitude and mean stresses (Fig. 8a). A typical uniaxial ratcheting response is shown in Fig. 9. In this figure, the axial strain is accumulating with cycles.

The first set of biaxial experiments involve symmetric axial strain-controlled cycles in the presence of constant internal pressure (Fig. 8b). A typical axial stress-strain and axial-circumferential strain responses from such an experiment is shown in Fig. 10. In these experiments, due to the presence of constant internal pressure, the circumferential strain ratchets with cycles.

The second set of biaxial experiments involved a *bow-tie* loading history as shown in Fig. 8c. This loading history resembles the history in a straight pipe subjected to cyclic bending and external pressure (Corona et al. [1996]). A constitutive model which can predict the bow-tie experiment responses is expected to be able to predict the responses of piping components. Experimental responses from a bow-tie experiment is shown in Fig. 11, in which the circumferential strain is ratcheting due to the presence of internal pressure. The third set of biaxial experiments involved a *reverse bow-tie* loading history (Fig. 8d). The material in these experiments also ratchets in the circumferential direction.

Theory

Constitutive models for rate-independent ratcheting responses of stable materials are studied in this research. All the models considered have the following two common features:

$$\text{Yield surface: } f(\underset{\sim}{\sigma}-\underset{\sim}{\alpha}) = \left[\frac{3}{2}(\underset{\sim}{s}-\underset{\sim}{a})\bullet(\underset{\sim}{s}-\underset{\sim}{a})\right]^{1/2} = \sigma_0 \qquad (1)$$

$$\text{Flow rule: } d\underset{\sim}{\varepsilon}^p = \frac{1}{H}\left\langle\frac{\partial f}{\partial \underset{\sim}{\sigma}}\bullet d\underset{\sim}{\sigma}\right\rangle\frac{\partial f}{\partial \underset{\sim}{\sigma}} \qquad (2)$$

where, $\underset{\sim}{\sigma}$ is the stress tensor, $\underset{\sim}{s}$ is the deviatoric stress tensor, $\underset{\sim}{\alpha}$ is the current center of the yield surface, $\underset{\sim}{a}$ is the current center of the yield surface in the deviatoric space, σ_0 is the size of the yield surface, which is constant for a stable material, and H is the plastic modulus. Other essential features of each of the models are briefly stated in the following.

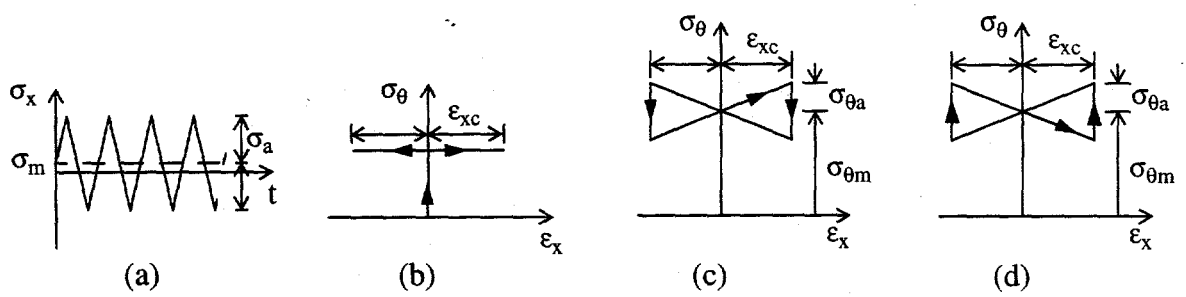

Fig. 8. Loading histories. (a) Uniaxial, (b) biaxial constant pressure, (c) biaxial bow-tie, (d) biaxial reverse Bow-tie.

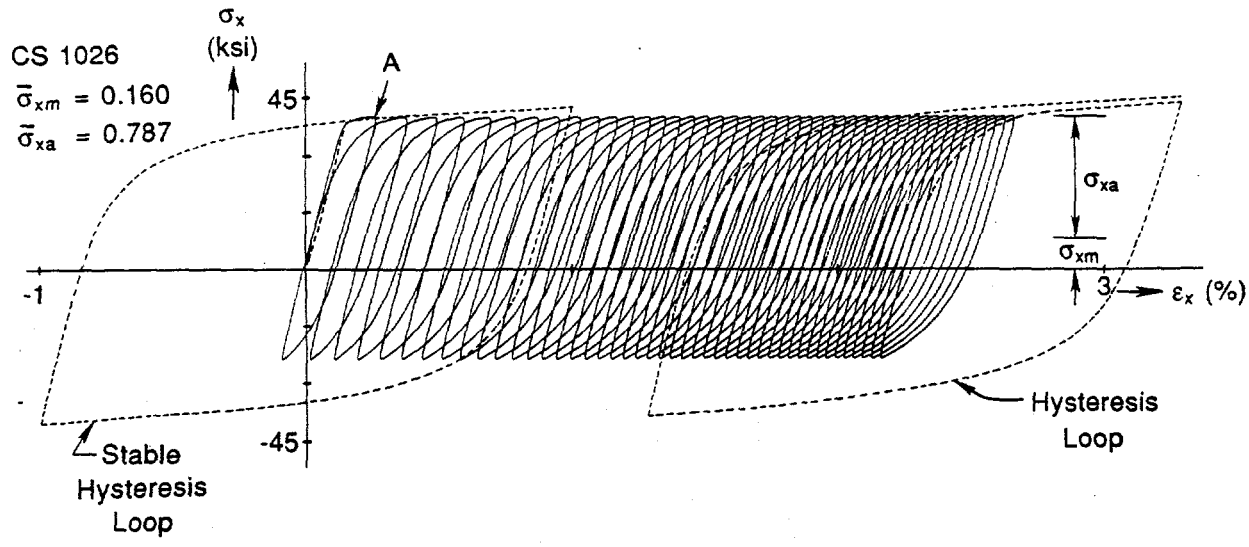

Fig. 9. Uniaxial strain ratcheting response for CS 1026 (From Hassan and Kyriakides [1992])

Chaboche Model

The evolution of the yield surface during a plastic loading increment is evaluated through translation of the yield surface using the kinematic hardening rule:

$$d\underset{\sim}{a} = \sum_{i=1}^{4} d\underset{\sim}{a}_i \ , \ d\underset{\sim}{a}_i = \frac{2}{3} C_i d\underset{\sim}{\varepsilon}^p - \gamma_i \underset{\sim}{a}_i dp \ , \quad dp = \left| d\underset{\sim}{\varepsilon}^p \right| \ , \ \text{for } i = 1, 2 \text{ and } 3$$

$$\text{and } d\underset{\sim}{a}_i = \frac{2}{3} C_i d\underset{\sim}{\varepsilon}^p - \gamma_i \underset{\sim}{a}_i \left\langle 1 - \frac{\bar{a}_i}{f(\underset{\sim}{\alpha}_i)} \right\rangle dp \frac{\left\langle \underset{\sim}{a}_i \bullet d\underset{\sim}{\varepsilon}^p \right\rangle}{\left| \underset{\sim}{a}_i \bullet d\underset{\sim}{\varepsilon}^p \right|}, \ \text{for } i = 4. \qquad (3)$$

Eq. 3 for $i = 4$ is slightly modified from that proposed by Chaboche [1991] to conform with the physical characteristics of a stable hysteresis loop. The plastic modulus H is evaluated using the consistency condition, $\dot{f} = 0$, kinematic hardening rule, Eq. 3, flow rule, Eq. 2, and the yield

surface equation, Eq. 1. Like the classical plasticity model, calculation of the plastic modulus H in this model is directly tied to the kinematic hardening rule.

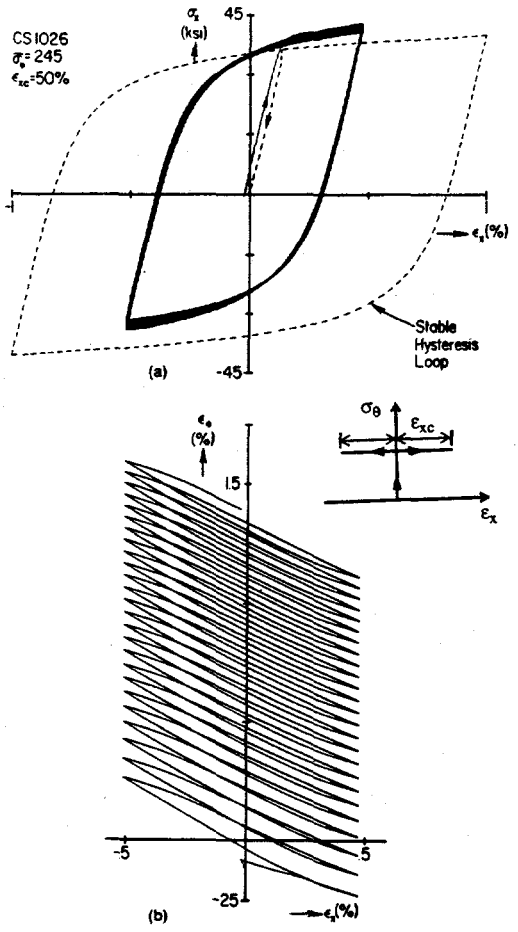

Fig. 10. Biaxial ratcheting in axial strain-symmetric cycling of a thin-walled tube at a constant internal pressure. (a) Axial stress-strain response, (b) circumferential strain ratcheting response (From Hassan et al.

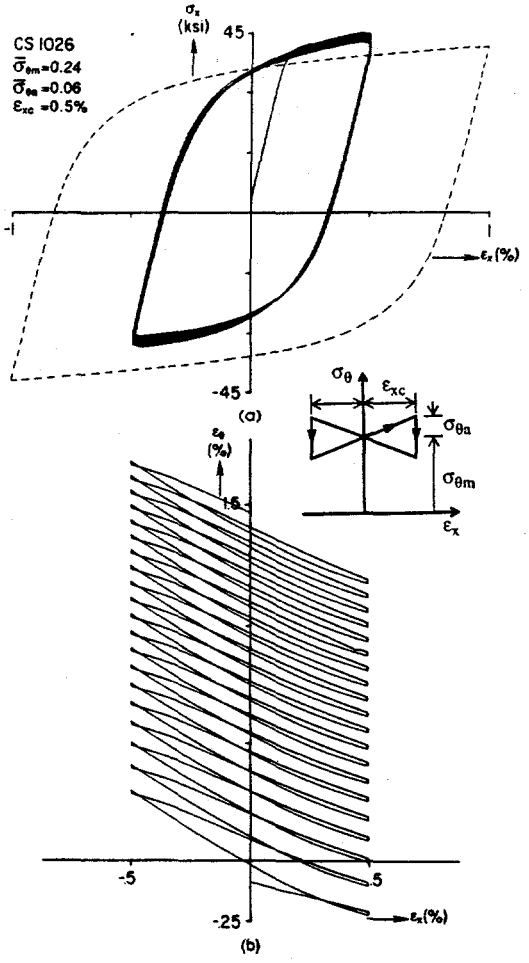

Fig. 11. Biaxial ratcheting from bow-tie loading history in the axial strain and circumferential stress space. (a) Axial stress-strain response, (b) circumferential strain ratcheting response (From Corona et al.

Guionnet Model

Here the kinematic hardening rule is proposed in the form:

$$d\underline{a} = mp_1^{m-1}\left[\left\{\frac{2}{3}C - \gamma_1(\underline{a}\bullet\underline{n})\right\}d\underline{\varepsilon}^p - (\gamma_2\alpha)\underline{a}dp\right],\quad \underline{n} = \frac{2}{3}\left(\frac{d\underline{\varepsilon}^p}{dp}\right) \tag{4}$$

$$\alpha = p_1^n = p_{1M}^n, \text{ for } p_1 = p_{1M},\ \alpha = p_{1M}^n\left(\frac{p_{1M}}{p_{1M}+p_1}\right)^{\beta}, \text{ for } p_1 \le p_{1M}\ ,$$

$$p_1 = \int_{I_K}^{M} dp \quad , \text{ and } \quad p_{1M} = \int_{I_{K-1}}^{I_K} dp$$

where, p_1 and p_{1M} are the accumulated plastic strains between the last reversal and current loading point and the last two reversals, respectively. The plastic modulus H is evaluated following the classical approach as discussed in the Chaboche model.

Ohno Model

This model proposed the kinematic hardening rule in the form:

$$d\underset{\sim}{\alpha} = \sum_{i=1}^{12} d\underset{\sim}{\alpha}_i, \quad d\underset{\sim}{\alpha}_i = \frac{2}{3} C_i d\underset{\sim}{\varepsilon}^p - \gamma_i \underset{\sim}{\alpha}_i \left\langle d\underset{\sim}{\varepsilon}^p \bullet \frac{\underset{\sim}{\alpha}_i}{f(\underset{\sim}{\alpha}_i)} \right\rangle \left(\frac{f(\underset{\sim}{\alpha}_i)}{C_i/\gamma_i} \right)^{m_i}. \tag{5}$$

The plastic modulus H is evaluated following the classical approach as discussed in the Chaboche model.

Dafalias-Popov Model

In this model the plastic modulus H is evaluated using a bounding surface concept and its evaluation is not directly dependent on the choice of the yield surface kinematic hardening rule. Implementation of the Dafalias-Popov model involves the following equations:

$$F(\underset{\sim}{\sigma} - \underset{\sim}{\beta}) = \left[\frac{3}{2} (\underset{\sim}{s} - \underset{\sim}{b}) \bullet (\underset{\sim}{s} - \underset{\sim}{b}) \right]^{1/2} = \sigma_b \quad \text{(bounding surface)}, \tag{6}$$

$$H = E_o^P + h\left(\frac{\delta}{\delta_{in} - \delta} \right), \quad h = \frac{a}{1 + b\left(\frac{\delta_{in}}{2\sigma_b} \right)^m}, \quad \delta = \left[\frac{3}{2} (\underset{\sim}{s} - \underset{\sim}{s}) \bullet (\underset{\sim}{s} - \underset{\sim}{s}) \right]^{1/2}. \tag{7}$$

The original Dafalias-Popov model simulates an eventual shakedown for uniaxial ratcheting. Hassan and Kyriakides [1994] developed a modified version to improve its ratcheting simulation. This improvement incorporates relaxation of the bounding surface through its kinematic rule using (see Eqs. 24, 25 and 26 in Hassan and Kyriakides [1994]):

$$E_b^P = E_o^P + C_r[(\underset{\sim}{b} \bullet \underset{\sim}{b})^{1/2} - \underset{\sim}{b} \bullet \underset{\sim}{n}]. \tag{8}$$

The Dafalias-Popov model provides the flexibility of adopting any chosen kinematic hardening rule. In this study, we started with adopting the original Armstrong-Frederick kinematic hardening rule.

Parameters of the Models

A set of model parameters was determined following the methods prescribed by the model considered and a single set were used for simulation of all the responses, both uniaxial and biaxial, to test the generality of that model.

Parameters used are: σ_0=18.8 ksi, E=26300 ksi, ν=0.302 (common to all the models)

Chaboche: C_1=60000, C_2=3228, C_3=455, C_4=15000;

γ_1=20000, γ_2=400, γ_3=11, γ_4=5000, $\bar{a}_4$=5

Guionnet: C=3450, γ_1=150, γ_2=20, m=0.8, n=0.075, β=0.4

Ohno: $C_{1\text{-}12}$ = 31940, 36214, 2520, 376, 11021, 4551, 3475, 2196, 857, 247, 98, 200;

$\gamma_{1\text{-}12}$ = 45203, 13944, 7728, 4955, 3692, 2135, 1230, 585, 295, 119, 50, 20;

m=0.45

Dafalias-Popov: σ_b= 38.66 ksi, a=71100, b=27, m=2, C/γ=140, C_r=10, E_0^p=274 ksi

Predictions

Predictions of all sets of ratcheting responses by the *Chaboche model* is plotted in Fig. 12. In the figures, the maximum strain in each cycle is plotted as a function of the number of cycles. The Chaboche model predicts the responses for all the uniaxial loading cases with reasonable accuracy (Figs. 12a,b). This performance is expected since most of the parameters of this model had been determined from a stable, uniaxial hysteresis curve. But this model overpredicts the ratcheting for all the biaxial loading cases (Figs. 12c,d,e,f).

Predictions from the *Ohno model* are shown in Fig. 13. Like Chaboche model, this model also predicts the ratcheting responses for all the uniaxial loading cases with reasonable accuracy (Figs. 13a,b). In this model all the parameters are also determined from a uniaxial stable hysteresis loop and hence this performance is expected. This model performs a little better for all the biaxial loading cases, compare to the Chaboche model, but the trend of overprediction persists (Figs. 13c,d,e,f).

The *Guionnet model* as shown in Figs. 14a,b fails to predict the uniaxial ratcheting responses. This model was found to have some divergence numerical problem when large ratcheting rates were considered. But, the model performs the best in predicting the first set of biaxial ratcheting responses (Figs. 14c,d). For the bow-tie loading case, this model overpredicts, whereas for the reverse bow-tie it underpredicts the ratcheting (Fig. 14e,f).

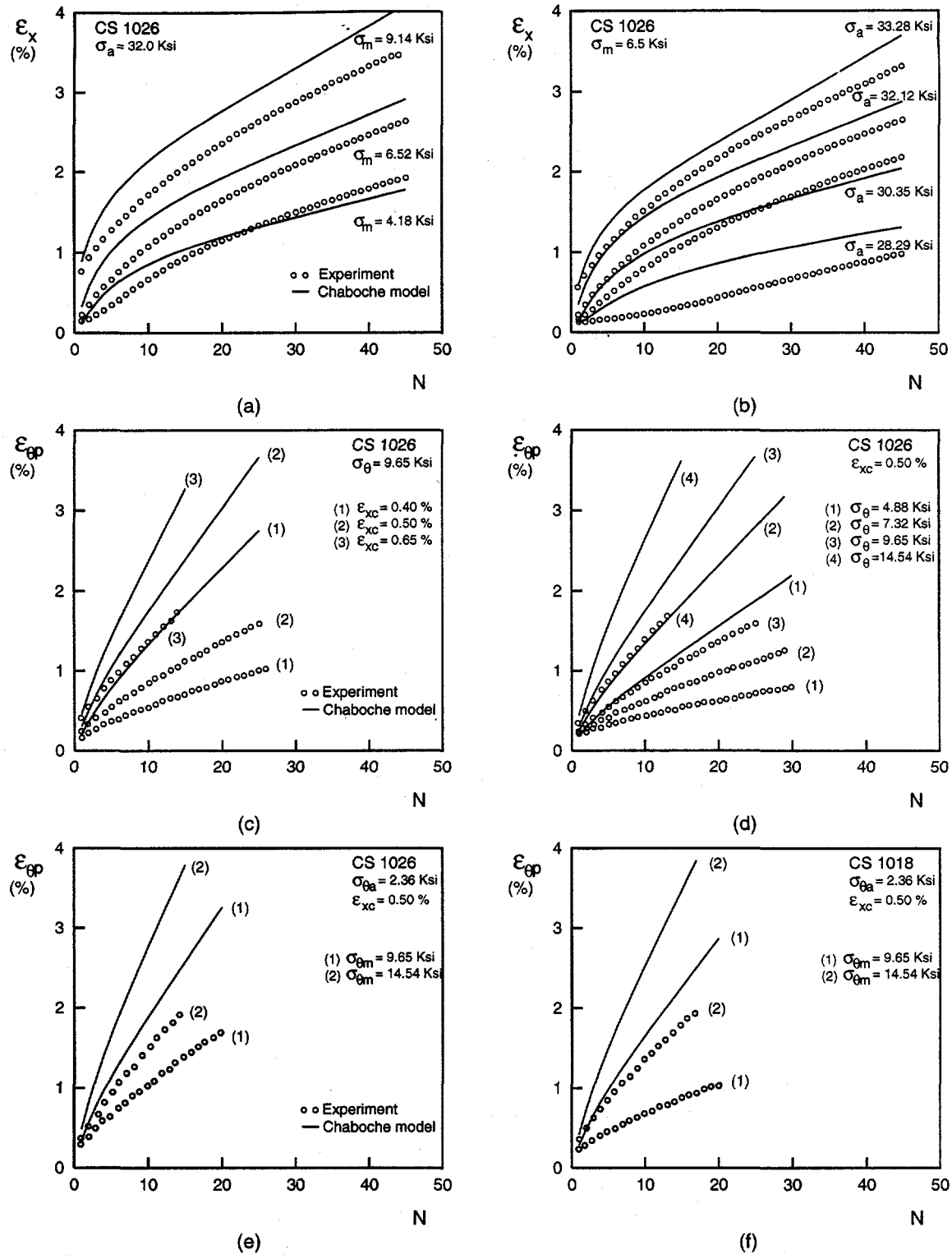

Fig. 12. Simulations for uniaxial, biaxial, bow-tie and reverse bow-tie ratcheting responses by the Chaboche model [1991].

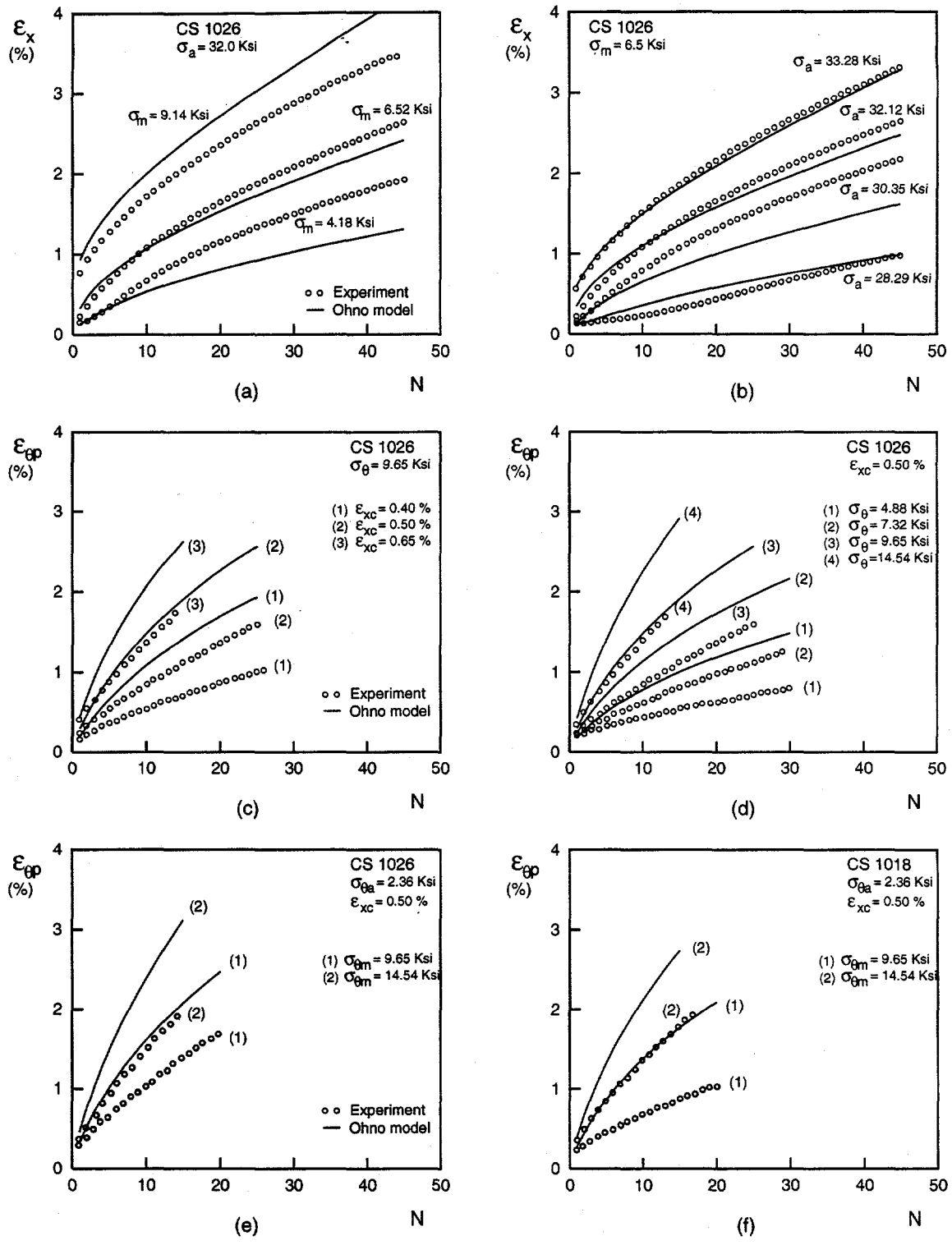

Fig. 13. Simulations for uniaxial, biaxial, bow-tie and reverse bow-tie ratcheting responses by the Ohno model [1993, 1997].

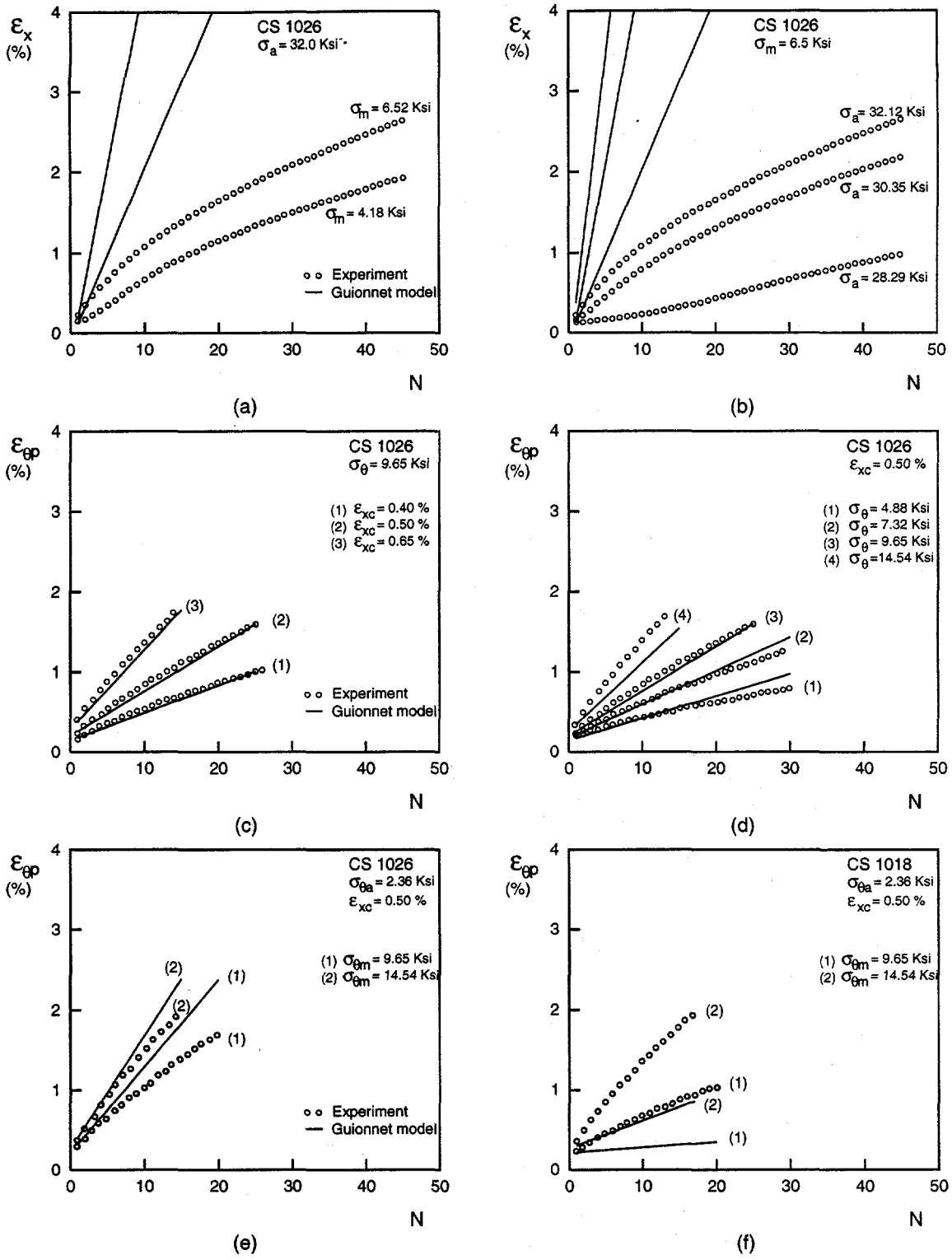

Fig. 14. Simulations for uniaxial, biaxial, bow-tie and reverse bow-tie ratcheting responses by the Guionnet model [1992].

Figure 15 shows the predictions by the modified *Dafalias-Popov* model (Hassan and Kyriakides [1994]). This model performs good in predicting both uniaxial (Figs. 15a,b) and first set of biaxial (Figs. 15c,d) ratcheting responses. This model's performances for the bow-tie and reverse bow-tie loading cases are similar to those of Guionnet model, overprediction and underprediction of ratcheting, respectively. Similar predictions were also reported by Corona et. al. [1996] using the modified Dafalias-Popov model and Armstrong-Frederick kinematic hardening rule.

It is observed that all the four models considered above fall short of predicting the ratcheting responses in a comprehensive and consistent way for the series of responses considered. Improvement to the Chaboche [1991, 1994] and the modified Dafalias-Popov model (Hassan and Kyriakides, 1994a) are attempted. The results obtained from the modified models are promising and reported below.

Improved Models

The Chaboche and Dafalias-Popov models were improved using the knowledge gained from the above evaluations. The improved models and their performances are discussed below.

Modified Model I

The Chaboche model [1991] was improved by modifying the kinematic hardening rule as follows:

$$d\underset{\sim}{a} = \sum_{i=1}^{4} d\underset{\sim}{a}_i \quad , d\underset{\sim}{a}_i = \frac{2}{3} C_i d\underset{\sim}{\varepsilon}^p - \gamma_i [\delta \underset{\sim}{a}_i + (1-\delta)(\underset{\sim}{a}_i \bullet \underset{\sim}{n})\underset{\sim}{n}] dp, \quad dp = \left| d\underset{\sim}{\varepsilon}^p \right| \quad , \text{ for } i = 1, 2 \text{ and } 3$$

$$\text{and } d\underset{\sim}{a}_i = \frac{2}{3} C_i d\underset{\sim}{\varepsilon}^p - \gamma_i [\delta \underset{\sim}{a}_i + (1-\delta)(\underset{\sim}{a}_i \bullet \underset{\sim}{n})\underset{\sim}{n}] \left\langle 1 - \frac{\bar{a}_i}{f(\underset{\sim}{\alpha}_i)} \right\rangle dp \frac{\left\langle \underset{\sim}{a}_i \bullet d\underset{\sim}{\varepsilon}^p \right\rangle}{\left| \underset{\sim}{a}_i \bullet d\underset{\sim}{\varepsilon}^p \right|}, \underset{\sim}{n} = \sqrt{\frac{2}{3}} \frac{d\underset{\sim}{\varepsilon}^p}{dp} \text{ for } i = 4.$$

Note that in the Chaboche kinematic hardening rule, Eq. 3, the term $\underset{\sim}{a}_i$ is replaced by $[\delta \underset{\sim}{a}_i + (1-\delta)(\underset{\sim}{a}_i \bullet \underset{\sim}{n})\underset{\sim}{n}]$ in the above modification. A parameter δ is added to this rule in order to introduce the effect of multiaxiality on ratcheting. These ideas are borrowed from the work of Delobelle et al. [1995].

All other schemes in this model remain the same as in the Chaboche model [1986, 1991, 1994]. As a result, the Chaboche model parameters remains the same for this model. The new parameter δ (= 0.2) is determined by fitting the ratcheting rate of one biaxial experiment. The predictions from the Modified Model I are shown in Fig. 16. Note that the uniaxial ratcheting predictions by the modified and Chaboche models are same (compare Figs. 12a,b to Figs. 16a,b). This shows that the above modification in the kinematic hardening rule does not effect uniaxial response simulation. By comparing Figs. 12c,d,e,f to Figs. 16c,d,e,f we find that the biaxial ratcheting simulations by the modified model are improved significantly.

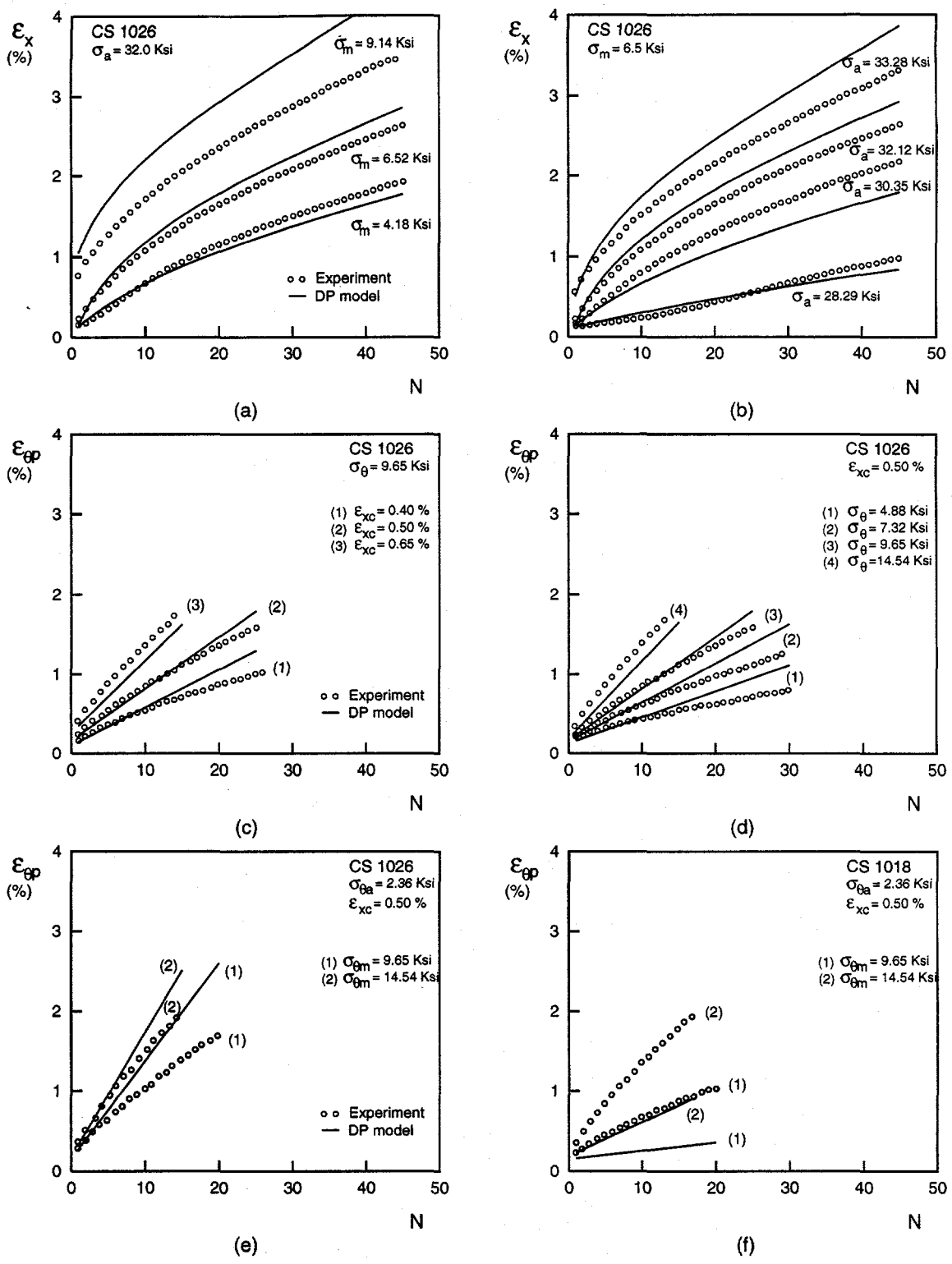

Fig. 15. Simulations for uniaxial, biaxial, bow-tie and reverse bow-tie ratcheting responses by the modified Dafalias-Popov model [Hassan and Kyriakides, 1994].

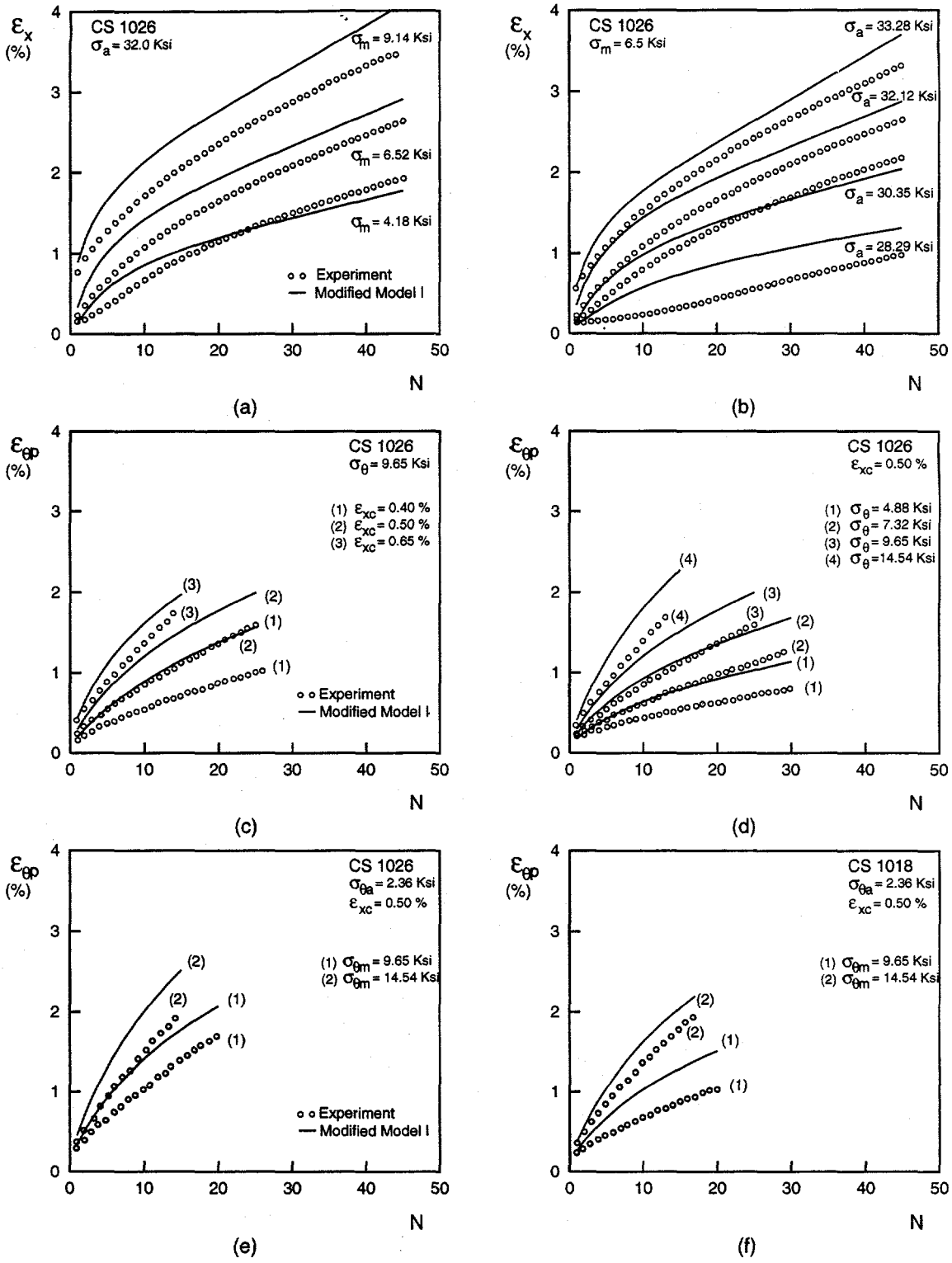

Fig. 15. Simulations for uniaxial, biaxial, bow-tie and reverse bow-tie ratcheting responses by the Modified Model I.

Modified Model II

The modification is obtained by combining the ideas from Dafalias-Popov [1976], Hassan and Kyriakides [1994] and Chaboche [1991, 1994]. The bounding surface formulation given by Eqs. (6), (7) and (8) is combined to the Chaboche type kinematic hardening rule with three decomposed terms as follows:

$$d\underline{\alpha} = \sum_{i=1}^{3} d\underline{\alpha}_i, \; d\underline{\alpha}_i = \frac{2}{3} C_i d\underline{\varepsilon}^p - \gamma_i \underline{\alpha}_i dp, \quad dp = \left| d\underline{\varepsilon}^p \right| \text{ , for } i = 1, 2 \text{ and } 3$$

Model parameters used for the predictions are:

$$\sigma_b = 38.66 \text{ ksi}, \; a = 71100, \; b = 27, \; m = 2, \; C_r = 10, \; E_0^p = 274 \text{ ksi}$$

$$C_{1\text{-}3} = 4800, 400, 140; \quad \gamma_{1\text{-}3} = 1200, 20, 1$$

The predictions from the *Modified Model II* are shown in Fig. 17. The uniaxial ratcheting predictions of this model are exactly the same as obtained from the Dafalias-Popov model (compare Figs. 15a,b and 17a,b). This is because the only difference between the two models is in the kinematic hardening rule adopted. In the Dafalias-Popov modeling scheme, the kinematic hardening rule does not have any effect on the uniaxial response predictions. The incorporation of the three decomposed Armstrong-Frederick kinematic hardening rules with the Dafalias-Popov model improves its predictions significantly for all the biaxial ratcheting responses.

IV. Improved Finite Element Programs

The Modified Models I and II will be incorporation into ANSYS and ABAQUS finite element programs in order to verify the performance of the improved models in simulating ratcheting responses in piping components. The incorporation of Model I is near completion.

V. Other Center Projects

Two Center projects have used or are planning to use the experimental facility develop in this research program. The project entitled "Experimental Investigation of Response of Unanchored Objects to Base Excitation" will perform shake-table tests to verify the analytically derived criteria for rest mode and the calculated sliding and rocking response of an unanchored body under base excitation.

Another project entitled "B Stress Indices Using Finite Element Analysis" has utilized data from elbow component tests in order to verify the finite element analysis results and review the ASME Code provisions.

The students from the above two projects have contributed in developing experimental facility of this project.

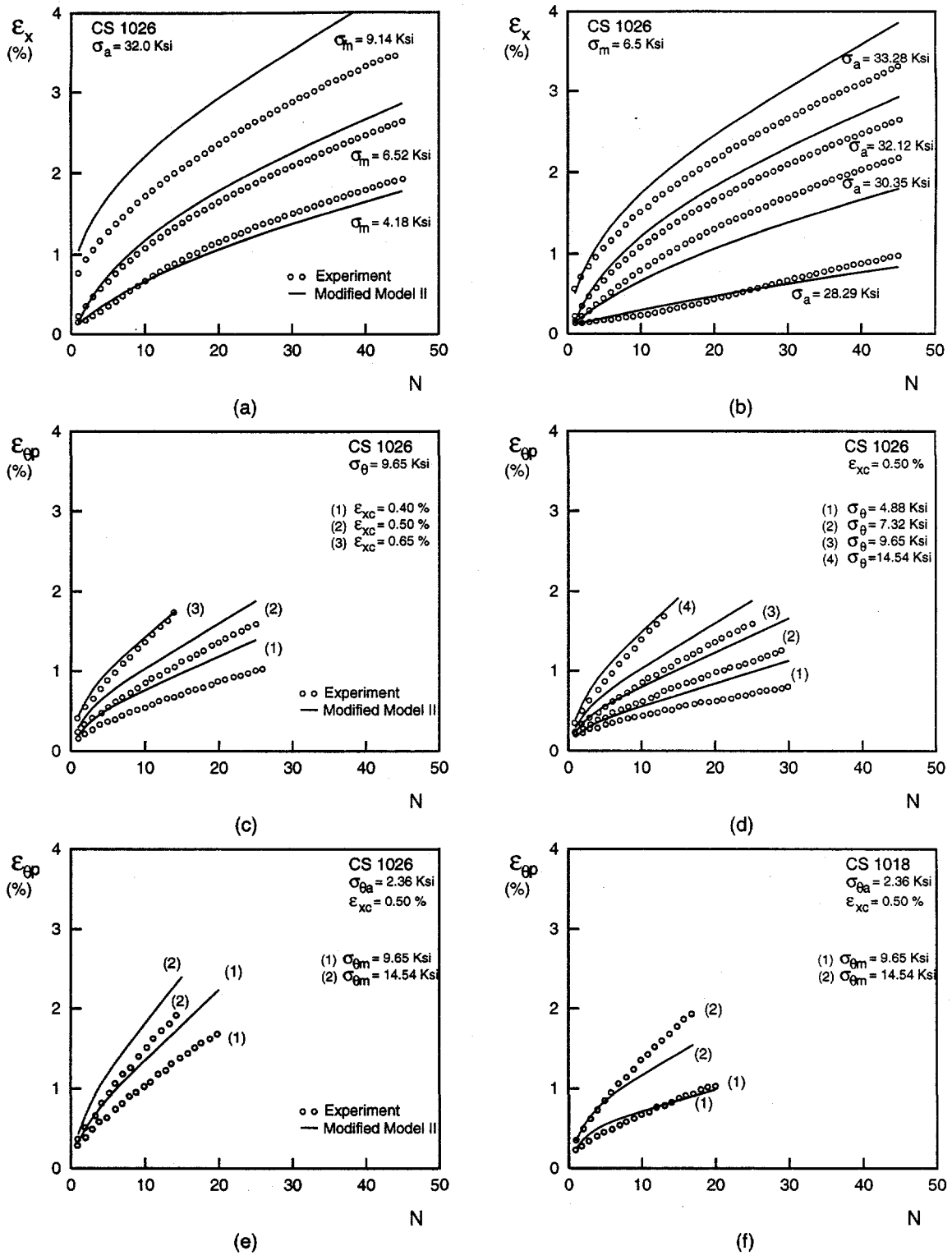

Fig. 17. Simulations for uniaxial, biaxial, bow-tie and reverse bow-tie ratcheting responses by the Modified Model II.

VI. Conclusion and Future Works

A state-of-the-art testing facility has been developed through this research project. This facility includes an one dimensional shake-table and a universal fatigue testing machine and will allow us to develop a systematic data set to study ratcheting. Quasi-static cyclic and seismic testing of straight and elbow piping components will be performed. A systematic testing program to study ratcheting has been developed. Some tests have already been performed and the rest will be completed by summer'99. Significant progress has been made in the area of constitutive modeling. Two modified models have been developed and their superior performance compare to existing models for simulating ratcheting is demonstrated.

The future research will first complete the experiments of the program developed. This involves conducting a systematic set of quasi-static cyclic testing on materials, and straight and elbow pipe components and seismic tests on straight and elbow pipe components. The acquired test data will be critically analyzed to understand the mechanisms of fatigue-ratcheting failure. The implementation of the improved constitutive models into widely used finite element programs, ANSYS and/or ABAQUS, will be completed. These improved analysis programs will be further improved, if needed, to simulate the ratcheting responses of piping components. The ASME Code provisions for ratcheting of piping components will be reviewed using the improved finite element program and acquired piping responses. Suggestions will be made to ASME Code committees for more rational methods for analysis of ratcheting in piping components. Simplified analysis methods for operability studies of piping components and systems will be developed.

REFERENCES

ANSYS, 1998, Version 5.7, ANSYS, Inc.

Chaboche, J.L. (1986), "Time-Independent Constitutive Theories For Cyclic Plasticity," International Journal of Plasticity, Vol. 2, pp. 149-188.

Chaboche, J.L. (1991), "On Some Modifications of Kinematic Hardening to Improve the Description of Ratcheting Effects," International Journal of Plasticity, Vol. 7, pp. 661-678.

Chaboche, J.L. (1994), "Modeling of ratchetting: evaluation of various approaches," European Journal of Mechanics, A/Solids, Vol. 13, pp. 501-518.

Corona, E., Hassan, T. and Kyriakides, S. (1996), "On the Performance of Kinematic Hardening Rules in Predicting a Class of Biaxial Ratcheting Histories," International Journal of Plasticity, Vol. 12, pp. 117-145.

Delobelle, P., Robinet, P. and Bocher, L. (1995), "Experimental Study and Phenomenological Modelization of Ratchet Under Uniaxial and Biaxial Loading on an Austenitic Stainless Steel," International Journal of Plasticity, Vol. 11, pp. 295-330.

Guionnet, C. (1992), "Modeling of Ratcheting in Biaxial Experiments," Journal of Engineering Materials and Technology, Vol. 114, pp. 56-62.

Hassan, T. and Kyriakides, S. (1992), "Ratcheting in Cyclic Plasticity, Part I: Uniaxial Behavior," International Journal of Plasticity, Vol. 8, p. 91-116.

Hassan, T., Corona, E. and Kyriakides, S. (1992), "Ratcheting in Cyclic Plasticity, Part II: Multiaxial Behavior," International Journal of Plasticity, Vol. 8, p. 117-146.

Hassan, T. and Kyriakides, S. (1994a), "Ratcheting of Cyclically Hardening and Softening Materials, Part I: Uniaxial Behavior," International Journal of Plasticity, Vol. 10, pp. 149-184.

Hassan, T. and Kyriakides, S. (1994b), "Ratcheting of Cyclically Hardening and Softening Materials, Part II: Multiaxial Behavior," International Journal of Plasticity, Vol. 10, pp. 185-212.

Hassan, T., Zhu, Y. and Matzen, V.C. (1998), "Improved Ratcheting Analysis of Piping Components," The International Journal of Pressure Vessels and Piping, Vol. 75, pp. 643-652.

Ohno, N. and Wang, J.-D. (1993a), "Kinematic Hardening Rules with Critical State of Dynamic Recovery, Part I: Formulations and Basic Features for Ratcheting Behavior," International Journal of Plasticity, Vol. 9, pp. 375-390.

Ohno, N. and Wang, J.-D. (1993b), "Kinematic Hardening Rules with Critical State of Dynamic Recovery, Part II: Application to Experiments of Ratcheting Behavior," International Journal of Plasticity, Vol. 9, pp. 391-403.

Ohno, N. (1997), "Current State of the Art in Constitutive Modeling for Ratcheting," Transactions of the 14th International Conference on SMiRT, Lyon, France.